AUSTRAL JOURNAL OF IMAGING
REVISTA CHILENA DE RADIOLOGÍA

PERMANYER

Check for updates

REVIEW ARTICLE

Skull base osteomyelitis: addressing the diagnostic challenge from the clinical-radiological perspective

Osteomielitis de base de cráneo: abordando el desafío diagnóstico desde la perspectiva clínico-radiológica

Camilo Muñoz-Núñez[1], Ivanko Grlica-Bahamondes[1], Andrés Miranda-Merchak[2], Ricardo Wenger-Carrasco[3], Marcelo López-Ramírez[4], and Rodrigo Araya-Rojas[5,6]*

[1]Faculty of Medicine, Medical Specialty Program in Radiology, Universidad Católica del Norte, Coquimbo; [2]Neuroradiology Unit, Hospital Barros Luco Trudeau, Metropolitan Region; [3]Neuroradiology Unit, Hospital Base Valdivia, Valdivia, Los Ríos; [4]Neuroradiology Unit, Hospital San José, Santiago; [5]Neuroradiology Unit, Hospital San Pablo de Coquimbo; [6]Neuroradiology Unit, Hospital San Juan de Dios de La Serena. Coquimbo. Chile

Abstract

Skull base osteomyelitis is a rare but serious and potentially life-threatening infection. Its nonspecific clinical presentation and the difficulty in isolating the causative microorganism make it a major diagnostic challenge, with imaging being essential for early suspicion. It typically presents in elderly patients with a history of diabetes mellitus *and an initial otic infection, usually due to Pseudomonas aeruginosa. In contrast, its atypical form usually affects middle-aged adults with a history of immunosuppression, who generally present with a rhinosinus infection caused by fungal or bacterial agents. After a review of recent literature and our own case series, we propose that imaging evaluation requires the complementary use of computed tomography and magnetic resonance imaging, whose key findings concentrate on four main elements: a primary infectious focus, phlegmonous changes in extracranial soft tissues, osteolysis, and bone marrow edema. The main difficulty lies in differentiating this process from a neoplastic one, for which certain imaging elements have been suggested. However, it is often not possible to rule out neoplasia with certainty, making an histopathological analysis essential.*

Keywords: *Osteomyelitis. Skull base. Neuroimaging. Computed tomography. Magnetic resonance imaging.*

Resumen

La osteomielitis de base de cráneo es una infección poco frecuente, pero grave y potencialmente mortal. Su cuadro clínico inespecífico y las dificultades para aislar un microorganismo causante la convierten en un gran desafío diagnóstico, donde el rol de las imágenes es fundamental para una sospecha precoz. Su presentación típica es en pacientes ancianos con antecedentes de diabetes mellitus *y una infección ótica inicial habitualmente por Pseudomonas aeruginosa. En contraste, su forma atípica suele afectar a adultos de mediana edad con antecedentes de inmunosupresión, quienes generalmente presentan una infección de origen rinosinusal por agentes fúngicos o bacterianos. Tras una revisión de la literatura reciente y de nuestra propia casuística, planteamos que la evaluación imagenológica requiere el uso complementario de tomografia computarizada y resonancia magnética, cuyos hallazgos clave se concentran en cuatro elementos principales: un foco infeccioso primario, cambios flegmonosos de los tejidos blandos extracraneales, osteólisis y edema de médula ósea. La principal dificultad radica en diferenciar este proceso de uno neoplásico, para lo cual se han sugerido ciertos elementos imagenológicos. No obstante, con frecuencia no es posible descartar una neoplasia con certeza, lo que hace imprescindible un estudio histopatológico.*

Palabras clave: *Osteomielitis. Base de cráneo. Neuroimagen. Tomografía computarizada. Resonancia magnética.*

Correspondence:
Camilo Muñoz-Núñez
E-mail: camilo.mznz@gmail.com

Date of reception: 14-10-2024
Date of acceptance: 17-02-2025
DOI: 10.24875/AJI.24000052

Available online: 24-10-2025
Austral J. Imaging. (Engl. ed.). 2025;31(4):206-216
www.resochradi.com

2810-708X / © 2025 Sociedad Chilena de Radiología. Published by Permanyer. This is an open access article under the CC BY-NC-ND license (https://creativecommons.org/licenses/by-nc-nd/4.0/).

Introduction

Skull base osteomyelitis (SBO) is a rare but serious and potentially fatal condition. It is an infectious process usually arising from an improperly treated otic or rhinosinus focus, which spreads to this anatomical region and most commonly involves the temporal, occipital, and sphenoid bones. Susceptible patients are usually elderly, diabetic, and immunosuppressed[1-3].

A nonspecific clinical picture, unremarkable laboratory anomalies, and difficulties in isolating a causative microorganism make it a major diagnostic challenge, requiring a high clinical suspicion. Added to this is the potential progression of the infectious process, possible recurrences, and treatment abandonment by some patients, which often requires addressing this disease at different stages of its evolution. Furthermore, imaging findings can be easily misinterpreted as a malignant neoplastic process, and it is necessary to complement different techniques for an adequate description of the extent of the disease[1,4-6]. Finally, unlike other anatomical sites, there are limitations in the surgical approach to debride the affected tissue, which restricts both therapeutic options and the collection of histological samples.

In a collaborative effort between different tertiary centers in northern, central, and southern Chile, we reviewed the available literature on the topic, emphasizing common imaging findings and pathways of dissemination. The literature analysis is accompanied by a total of 12 representative cases that exemplify the main anomalies described in this pathology.

Anatomical review

The skull base corresponds to the lower portion of the neurocranium. It presents a complex anatomy, composed of the frontal, temporal, occipital, ethmoid, and sphenoid bones. From an endocranial perspective, it can be divided into three regions: the anterior, middle, and posterior cranial fossae. The first two are bounded by the posterior margin of the lesser wings of the sphenoid, the anterior clinoid apophyses, the tuberculum sellae, and the anterior margin of the greater sphenoid wings. The separation between the middle and posterior cranial fossae is determined by the superior margin of the petrous portion and the dorsum sellae (Fig. 1).

The complexity of this anatomical region lies in the confluence of numerous neurovascular structures, which pass through different foramina and canals that communicate with the extracranial spaces. In the middle cranial fossa, the cavernous sinuses stand out, formed by venous plexuses that are located on both sides of the midline in relation to the body of the sphenoid. These vascular structures are crossed by the homonymous portions of the internal carotid arteries, the oculomotor (CN III) and trochlear (CN IV) nerves, the ophthalmic (V1) and maxillary (V2) divisions of the trigeminal (CN V) nerves, and the abducens nerve (CN VI). At the orbital apex, the optic nerve (CN II) and the ophthalmic artery run towards the orbit through the optic canal, while the III, IV, and IV pairs, and the V1 division of the trigeminal nerve, do so by crossing the superior orbital fissure more laterally. The maxillary branch of the trigeminal nerve (V2) exits the middle cranial fossa via the foramen rotundum and enters the pterygopalatine fossa, while the mandibular branch (V3) does the same through the foramen ovale towards the infratemporal fossa. The internal carotid artery ascends through the carotid canal in the petrous portion of the temporal bone to enter the middle cranial fossa, while the foramen spinosum provides passage for the middle meningeal artery and vein. The internal auditory canal is traversed by the facial (CN VII) and vestibulocochlear (CN VIII) nerves, while the abducens and trigeminal nerves travel from their origin in the brainstem through Dorello's canal and Meckel's cavum, respectively, to reach the cavernous sinus. In the posterior cranial fossa, the jugular foramen exits the glossopharyngeal nerve and the inferior petrosal sinus in its *pars* nervosa, while the internal jugular vein, vagus nerve, and accessory nerve pass through its *pars* vascularis[7].

A structure that requires special mention in the anatomical description is the clivus, a bony formation situated between the foramen magnum and the hypophyseal fossa that originates from the fusion of the basisphenoid and basiocciput in adolescence. Its central location at the base of the skull, as well as a significant trabecular component, determine its frequent involvement by this infectious process, both in cases of otic and rhinosinus origin[1,4].

The temporal bone, and particularly the ear, are anatomical structures commonly affected in SBO. Although it is not the objective of this publication to describe them in all their complexity, it is worth highlighting some important anatomical landmarks for understanding this pathology. Santorini fissures feature in the external auditory canal (EAC), small openings located in the floor of its fibrocartilaginous component that constitute potential dissemination pathways toward the temporal bone for both infectious and neoplastic processes[1,8].

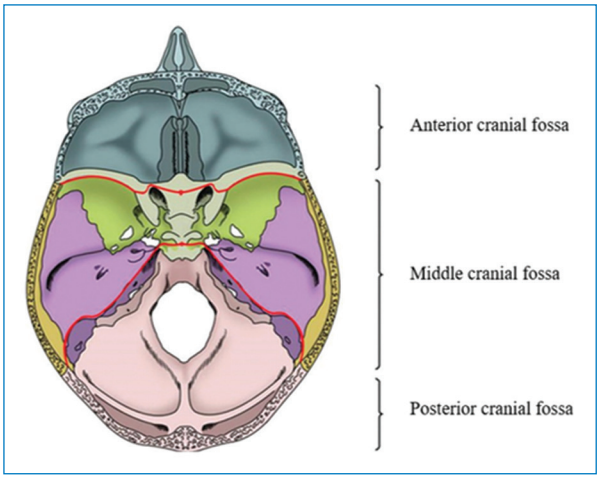

Figure 1. Anatomical division of the skull base. From an endocranial view, the skull base can be divided into three regions: the anterior, middle, and posterior cranial fossae. The first two are bounded by the posterior margin of the lesser wings of the sphenoid, the anterior clinoid processes, the tuberculum sellae, and the anterior margin of the greater sphenoid wings. The middle and posterior cranial fossae are separated by the superior margin of the petrous portion and the dorsum sellae.

Regarding the petrotympanic portion, it is worth highlighting the stylomastoid foramen, an opening located on its posteroinferior surface that provides exit for the CN VII, constituting a reference point for assessing early soft tissue involvement in SBO. Also located on the posteroinferior aspect of this portion are the aforementioned carotid canal and jugular foramen, in addition to the styloid process. The latter constitutes a fundamental anatomical landmark where the musculoligamentous structures that comprise Riolan's bundle insert, an anatomical boundary that subdivides the parapharyngeal space of the neck into the pre- and retrostyloid spaces[9].

Finally, in the mastoid portion of the temporal bone, the mastoid notch stands out, a deep bony indentation located on the medial aspect of its exocranial surface, which provides the origin site for the posterior belly of the digastric muscle, another important reference when describing the early involvement of the fatty planes secondary to an SBO[10].

Clinical findings and diagnostic approach

Although the symptoms are usually nonspecific and subacute, two main presentations have been described. Typical SBO occurs in elderly patients with a history of diabetes mellitus, who initially present with an ear infection manifested by otalgia and otorrhea, as well as hearing loss and paralysis or facial pain in the most severe cases[4]. In this group, the most frequently isolated microorganism is *Pseudomonas aeruginosa*, followed by *Staphylococcus aureus* and fungal agents, although the infection is often of polymicrobial cause[1,2,4]. In contrast, atypical SBO presents more commonly in middle-aged patients with a history of diabetes mellitus or other immunosuppressive conditions, such as human immunodeficiency virus (HIV) infection or chronic corticosteroid use, among the most frequent. These patients most commonly present with a rhinosinus infection characterized by facial pain, rhinorrhea, fever, and headache; odontogenic infections and patients without a verifiable primary focus are also included within this group. In atypical SBO, *S. aureus* is slightly more prevalent than *P. aeruginosa* and fungal agents[4]. In both types of SBO, patients may present with prolonged periods of poor general condition and weight loss, which also contribute to the initial clinical suspicion of a malignant neoplastic process.

After age, diabetes mellitus is the most commonly described predisposing factor[11]. Given the combination of immune dysfunction and microvascular angiopathy, this is an ideal scenario for infection by *P. aeruginosa*, a gram-negative bacterium whose virulence is associated with angioinvasion and thrombosis of the microvasculature[4]. In our series, the average age was 60 years, with 9 of the 12 patients being older adults. Seven patients had a history of type 2 diabetes mellitus, most of whom were insulin-requiring, with an average glycosylated hemoglobin of 9.7%, reflecting a state of metabolic decompensation of the disease. In nine cases, the initial focus of infection was otic, while three patients with an average age of 48 years had an atypical presentation, one of them with a history of promyelocytic leukemia and another with HIV; the latter manifested with simultaneous otic and sinus infections.

The isolation of a causative microorganism provides high diagnostic certainty; however, given the availability of previous antibiotic treatments and the difficulty in obtaining an adequate sample, this is often not possible. Djalilian et al.[12] reported eight cases of SBO, all with negative cultures, and other series have reported up to 70% of patients without an isolated microorganism[13], therefore it is not uncommon for antibiotic and antifungal treatment to be indicated empirically. However, the differential diagnosis with a neoplastic process based solely on clinical and radiological elements is usually insufficient, making a histopathological study advisable in

most cases, which in addition to ruling out a neoplastic process enables the detection of microorganisms using universal polymerase chain reaction techniques or direct visualization of fungal components, among others. This eventually allows for the indication of antibiotic and antifungal therapy with specific coverage, which is the ideal scenario considering that prolonged courses of treatment are generally required[1,2,14]. In our series, a biopsy sample was obtained in seven cases ruling out malignancy, with a chronic inflammatory process being the most frequently reported histopathological finding. Additionally, the infectious agent was isolated in five patients, corresponding to *Klebsiella pneumoniae* in one case, *S. aureus* as the sole agent in one case, *S. aureus* associated with *Enterobacter cloacae* and *Aspergillus niger* in one case, and *P. aeruginosa* in two cases. In two of the three patients with atypical SBO, the biopsy detected non-septate hyphae in the respective rhinosinus and palatine mucosa samples, suggesting a diagnosis of mucormycosis. One of them simultaneously presented a positive nasal cavity culture for *A. niger* and *E. cloacae*, as previously mentioned. In the remaining cases, the diagnosis was based primarily on clinical history and imaging findings, including a 6-year-old patient who presented with a brainstem abscess as a complication (Table 1).

Imaging findings

The imaging study is essential for a timely diagnosis of SBO, as well as allowing the selection and guiding the acquisition of histopathological specimens. An accurate radiological description of the extent of the disease requires complementary evaluation with computed tomography (CT) and magnetic resonance imaging (MRI), both performed with intravenous contrast. CT provides better delimitation of the initial cortical erosions, while MRI is superior in detecting early findings, such as bone marrow edema, and allows for better evaluation of soft tissue involvement, including the involvement of different fatty planes[1,4,6,15].

After analyzing the literature and our own case series, it is possible to conclude that the imaging findings are concentrated in four main elements: anomalies characteristic of the primary infectious focus, phlegmonous changes in the extracranial soft tissues, osteolysis, and bone marrow edema.

Primary infectious focus

In typical SBO, the initial infectious focus is usually otic, with involvement of the external ear being more common, which can be seen on CT and MRI as edema of the auricle associated with thickening and enhancement of the EAC walls, with possible occlusion of its lumen[1,4] (Fig. 2). Other initial infections include acute otitis media and mastoiditis, the latter characterized by opacification of the mastoid air cells and erosion of their septa[1]. Given the proximity of the EAC to its exit from the skull base, one of the most frequently affected cranial nerves is the VII nerve, especially when the stylomastoid foramen or mastoid process is involved. The progression of the infectious process can also reach the VIII cranial nerve in the internal auditory canal, resulting in sensorineural hypoacusia[4,9].

In atypical SBO, the primary focus is usually an invasive rhinosinus infection characterized by inflammatory changes in the soft tissues of the paranasal sinuses, which may or may not be enhanced depending on the infectious agent involved. Erosion of the bony margins is also recognized, with involvement of the sphenoid sinuses being more common in atypical SBO[1,4,11] (Fig. 3).

Phlegmonous changes in extracranial soft tissue

A precise histopathological definition of this component is complex, as it reflects an intermediate inflammatory state between soft tissue edema and outright abscess formation. On CT, it is seen as increased density and enhancement of the fat and muscle planes, while on MRI, soft tissues will present hypo- to isosignal on T1-weighted sequences and iso- to hypersignal on T2-weighted images, with varying degrees of diffusion restriction and heterogeneous enhancement after gadolinium administration. The latter constitutes the main element of differentiation from a constituted abscess, whose enhancement is typically peripheral[4].

In typical SBO, these phlegmonous changes usually extend from the soft tissues of the EAC through the Santorinian canals toward the temporal bone, from where they reach the extracranial fat planes adjacent to the stylomastoid foramen and medial to the digastric muscle[4,9] (Fig. 4). Mejzlik et al.[9] retrospectively analyzed different clinical and radiological variables that could predict the presence of SBO, among which inflammatory changes related to the stylomastoid foramen were the only variable that presented statistical significance. From this point, the anomalies can extend in different directions through the soft tissues situated below the base of the skull, the most common being the anteromedial propagation vector. The latter

Table 1. Summary of the patients' clinical and epidemiological characteristics

Age (years)	Medical history	HbA1c (%)	Origin	Cultures	Biopsy
98	Occlusive arterial disease, CKD IV	-	Otic	Negative	-
87	No medical history	-	Otic	Negative	-
72	IR 2DM, HTN	8.0	Otic	*Staphylococcus aureus*	Negative for neoplasia
71	IR 2DM, HTN, atrial fibrillation	10.1	Otic	Negative	Negative for neoplasia
70	2DM, HTN, hypothyroidism, right cholesteatoma	11.2	Otic	*Pseudomonas aeruginosa*	-
68	IR 2DM, HTN	9.2	Otic	*Pseudomonas aeruginosa*	Negative for neoplasia
67	IR 2DM, HTN	9.1	Otic	Negative	Negative for neoplasia
61	IR 2DM, HTN, poliomyelitis sequelae, cognitive impairment	7.2	Otic	Negative	Negative for neoplasia
6	Obesity	-	Otic	Negative (brainstem abscess)	-
61	IR 2DM, HTN, obesity, hypothyroidism, CKD IV, lacunar ischemic CVA	13	Sinus	*Aspergillus niger, Staphylococcus aureus, Enterobacter cloacae*	Non-septate hyphae suggestive of Mucorales
44	Acute promyelocytic luekemia	-	Sinus	*Klebsiella pneumoniae*	Non-septate hyphae suggestive of Mucorales
38	HIV, cutaneous Kaposi's disease, syphilis	-	Otic and sinus	Negative	-

CVA: cerebrovascular accident; IR 2DM: insulin-requiring type 2 diabetes mellitus; CKD: chronic kidney disease; HbA1c: glycated hemoglobin; HTN: hypertension (high blood pressure); HIV: human immunodeficiency virus.

encompasses the poststyloid (or carotid) space and the soft tissues related to the petroclival synchondrosis and the Eustachian tube, reaching the prevertebral musculature (*longus capiti, longus colli*, and anterior *rectus capitis* muscles), the nasopharynx, and eventually crossing contralaterally. Less frequently, it can also progress anteroinferiorly, entering the parotid, masticator, and prestyloid spaces, or inferomedially simultaneously toward the jugular foramen (Fig. 5). Involvement of the latter may be associated with neuropathies of the IX, X and XI nerves[1,4,9] (Fig. 6).

As previously mentioned, in atypical SBO, the changes begin in the paranasal sinuses, with the sphenoid bone usually being the epicenter of the disease. From this point, inflammatory changes usually spread to the central bone component of the skull base, primarily affecting the clivus, as well as the adjacent neurovascular canals and foramina of the middle and posterior cranial fossa. In particular, obliteration of the pterygopalatine fossa and the periantral adipose tissue is characteristic of invasive sinusitis associated with atypical SBO[1,4,16] (Fig. 3).

Osteolysis

CT imaging is of particular importance in this finding. The acquisition of submillimeter slices in the bone algorithm allows for multi-plane image reconstruction and a detailed assessment of the bone structure. The infectious process, which initially affects the soft tissues, spreads through the Haversian bone system, causing erosion of the bone cortex. It then enters the medullary canal and causes demineralization of the trabecular bone, which eventually leads to the formation of bony tracts and sequestrums (Fig. 3). These changes can be subtle and, together with the effacement of fat planes, often constitute the only clue to a SBO in the initial CT evaluation.

In typical OBC, the key areas to evaluate, apart from the bony EAC, are the mastoid tip, the temporomandibular joint, the petrous apex, the petroclival fissure, the jugular foramen, and the clivus (Fig. 7). In contrast, in atypical OBC, there is often evidence of invasive sinusitis with cortical erosions of the paranasal sinuses, particularly the sphenoid sinuses and ethmoid air cells, followed by changes along the clivus and the greater

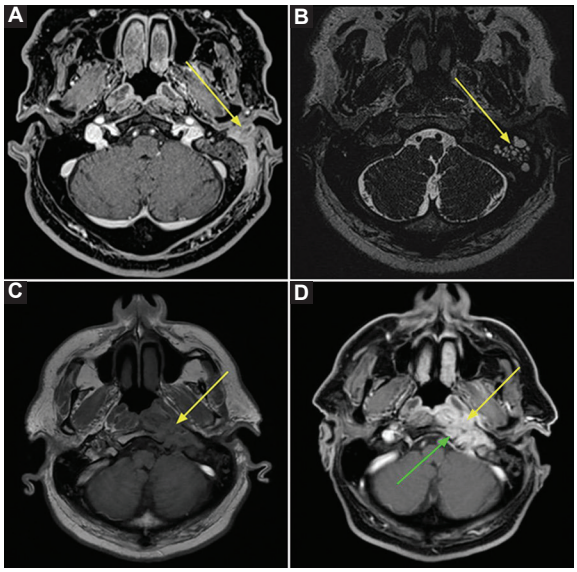

Figure 2. Primary otic focus (typical skull base osteomyelitis). A 67-year-old patient with a history of diabetes mellitus and a 1-month history of otalgia, vertigo, and hearing loss, for which a brain and ear MRI was indicated. The post-contrast T1-weighted sequence with fat saturation revealed thickening and hyperenhancement of the left external auditory canal (arrow in **A**) associated with fluid occupation of the ipsilateral mastoid air cells, evidenced on a high-resolution T2-weighted sequence (arrow in **B**). Pre- and post-contrast T1 images also revealed hyposignal (arrow in **C**) and heterogeneous enhancement (yellow arrow in **D**) of the extracranial soft tissues adjacent to the otomastoid region, with anteromedial extension towards the prevertebral musculature and nasopharyngeal mucosa; at this level, it obliterates the distal end of the Eustachian tube and Rosenmüller's fossa. Medially, it also occupies the jugular foramen in its *pars* nervosa and vascularis, with hyperenhancement of the adjacent trabecular bone (green arrow in **D**). Physical examination of the patient revealed involvement of the left cranial nerves IX, X, XI, and XII.

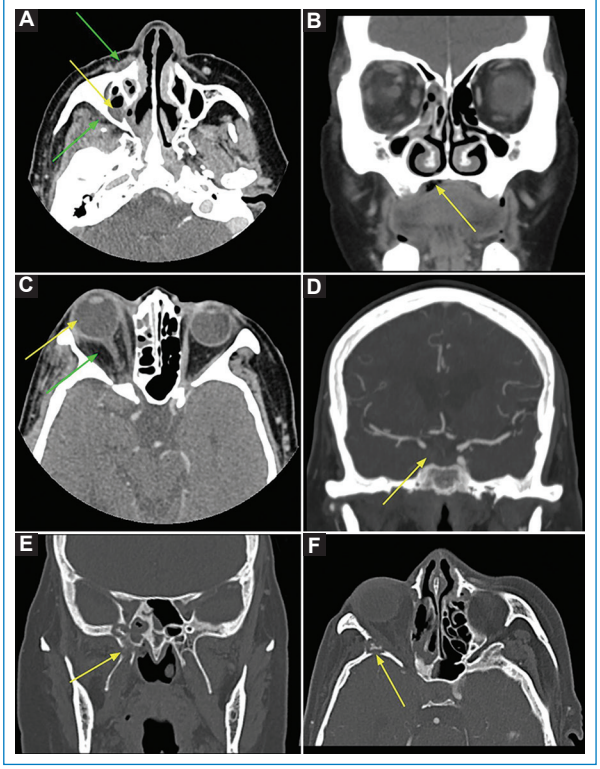

Figure 3. Primary rhinosinusal focus (atypical skull base osteomyelitis). A 61-year-old patient with a history of decompensated insulin-requiring type 2 diabetes mellitus was admitted for suspected fungal sinusitis. Initial computed tomography (CT) revealed partial mucosal occupation of the right ethmoid airways, nasal cavity, sphenoid sinus, and maxilla (yellow arrow in **A**); the latter was associated with inflammatory changes in the soft tissues adjacent to the anterior wall of the maxillary sinus and the retroantral fat plane (green arrows in **A**). In addition, mild emphysema and hypoenhancement of the palatine mucosa on the right were identified (arrow in **B**). The changes extended through the pterygopalatine fossa, via the inferior orbital fissure into the extra- and intraconal adipose tissue of the right orbit (green arrow in **C**), causing moderate proptosis of the eyeball (yellow arrow in C). CT angiography showed an absence of representation of the right internal carotid artery in its intracranial segments, consistent with secondary vascular compromise (arrow in **D**). Although the initial study did not reveal bone changes, a follow-up CT scan revealed osteolytic changes in the body and wings of the sphenoid bone on the right (arrow in **E**), with the formation of a bony sequestrum at the level of the greater wing (arrow in **F**).

and lesser wings of the sphenoid, with possible involvement of the foramina of the middle cranial fossa. This latter aspect may be crucial to consider potential neurovascular complications in the initial evaluation[14].

Bone marrow edema

Bone marrow edema is a significant anomaly in osteomyelitis of any part of the skeleton, and is the earliest imaging finding at presentation. In SBO, this alteration, which is usually evident on MRI, may be more difficult to detect given the smaller size of the bone components in this anatomical region, as well as their respective medullary cavities. It is characterized by hyposignal of the bone marrow on T1-weighted sequences, which also appears hyperintense on STIR sequences, and with heterogeneous hyperenhancement

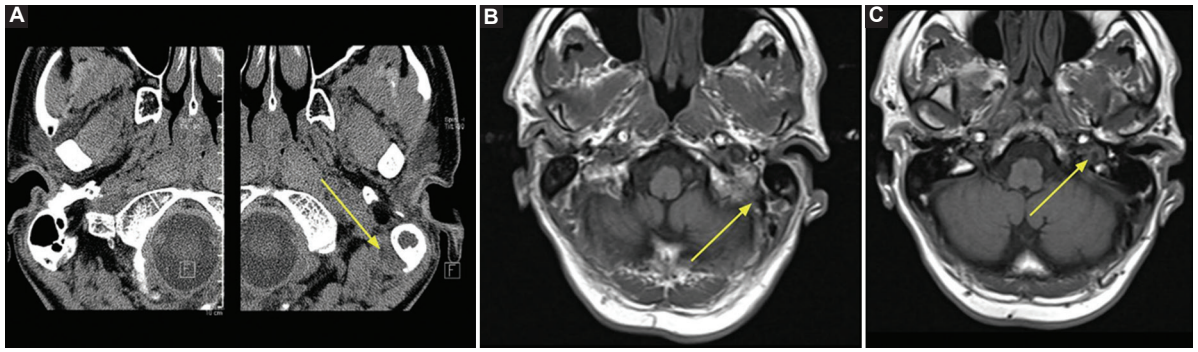

Figure 4. Early soft tissue changes. A 12-year-old patient with clinically diagnosed otitis suppurativa. The admission CT scan revealed involvement of the extracranial soft tissues adjacent to the left mastoid, in this particular case characterized by effacement of the fat plane adjacent to the mastoid notch, a space that also borders the groove for the occipital artery (arrow in **A**). This finding led to the request for an MRI, which confirmed the T1 hiposignal of the adipose tissue at this level (arrow in **B**) and also showed a prominence of the right jugular tubercle, with low T1 signal, indicating bone marrow edema (arrow in **C**).

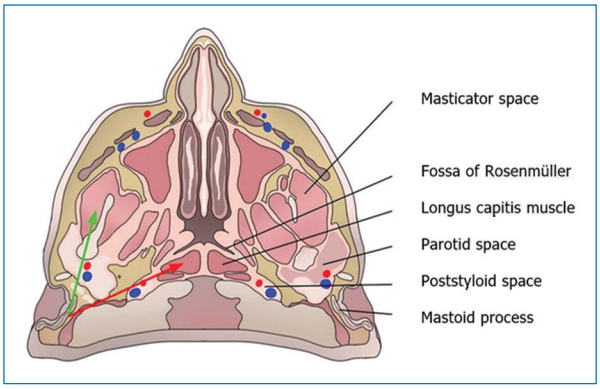

Figure 5. Pathways of dissemination for typical skull base osteomyelitis. The various anomalies, particularly phlegmonous changes in the extracranial soft tissues, often extend from the otomastoid region in different directions, as indicated by the arrows in this schematic figure on the axial plane at the level of the nasopharynx. The most common spread vector is anteromedial (red arrow), with involvement through the soft tissues below the skull base at the level of the petroclival region, the poststyloid (carotid) space, the prevertebral muscles, and the nasopharynx. They may also progress simultaneously anteroinferiorly, entering the parotid, masticator, and parapharyngeal spaces (green arrow), or inferomedially toward the jugular foramen (not shown).

after gadolinium administration on fat-saturated T1 images. The progression of the infection can cause necrosis of the bone marrow tissue, which on rare occasions leads to the formation of an abscess, characterized mainly by restricted diffusion of its contents and peripheral enhancement on contrast-enhanced images. Bone marrow edema is usually detected in the trabecular component of the clivus, followed by the petrous apex, the greater and lesser wings of the sphenoid, the rest of the occipital and temporal bones, and the craniocervical junction[1,4] (Fig. 8).

Differential diagnosis

The main diagnostic dilemma of SBO is its differentiation from a neoplastic process. Some tumors, such as nasopharyngeal carcinoma and EAC carcinoma, can also infiltrate the skull base, with similar clinical and radiological characteristics[6]. Other tumors, such as lymphoma, myeloma, or metastatic disease, are occasionally accompanied by a pertinent clinical history and other extracranial findings that indicate the presence of an underlying multifocal disease. A number of imaging elements have been described in the literature that may be useful in this differentiation:

- Most primary invasive neoplasms of the skull base have a dominant soft tissue mass or nodule, which may secondarily infiltrate bony structures. This lesion is usually identifiable and reasonably measurable on high-resolution MR images, especially on fat-saturated contrast-enhanced T1-weighted sequences.
- The malignant neoplastic processes usually displace or replace different anatomical structures, whereas in SBO, the inflammatory changes tend to occupy different tissue planes, without significant alteration of the normal anatomical architecture.
- It has been described that in SBO, MRI reveals a greater bone involvement compared to findings on

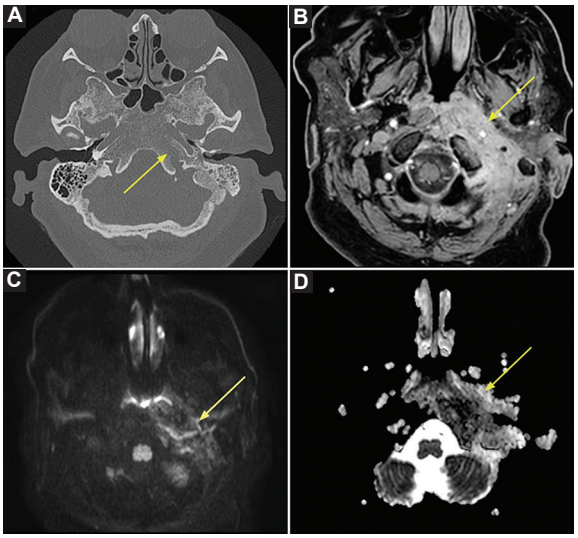

Figure 6. Phlegmonous changes in extracranial soft tissues. A 61-year-old patient with a history of type 2 diabetes mellitus and sequelae of poliomyelitis presented to the emergency department with a 5-month history of otorrhea, periauricular pain, and hearing loss. An initial evaluation with a computed tomography scan of the ears revealed signs of left otitis externa and otomastoiditis associated with erosive bone changes at the base of the skull, centered on the *pars* nervosa of the jugular foramen and the ipsilateral petroclival joint (arrow in **A**). Magnetic resonance imaging of the brain and ears performed 6 days later showed inflammatory changes in the extracranial soft tissues, extending from the otomastoid region in an anteromedial direction, occupying the carotid and retropharyngeal spaces, and involving the prevertebral muscles. These alterations are characterized by hyperenhancement after gadolinium administration on T1 sequences with fat saturation (arrow in **B**) and areas of diffusion restriction in their thickness (arrows in **C** and **D**).

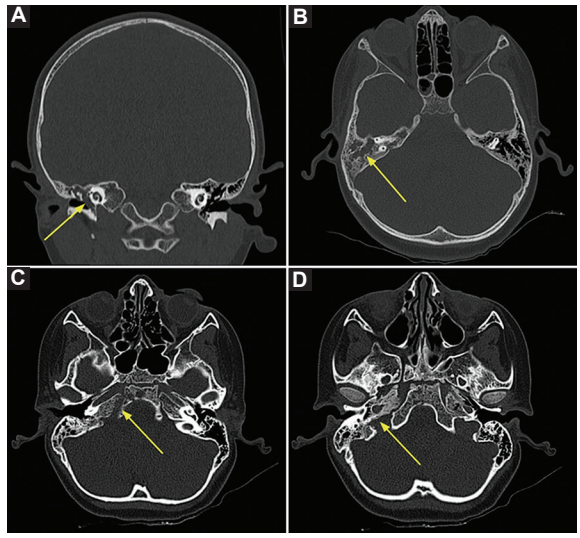

Figure 7. Osteolysis. A 6-year-old patient presented with a subacute condition characterized by otalgia and retroauricular pain. On the admission brain CT scan, the bone algorithm evaluation allowed for the characterization of the middle ear occupation (arrow in **A**) and the right mastoid air cells, with coalescence of the latter, indicating osteolysis of their septa (arrow in **B**). The patient was discharged after completing antibiotic treatment, returning to the clinic 40 days later due to a recurrence of symptoms, in addition to weakness in the left side of the body. A repeat brain CT scan revealed osteolytic changes in the petroclival region (arrow in **C**) and the right jugular foramen (arrow in **D**), suggestive of skull base osteomyelitis, which was later confirmed by MRI.

CT, whereas in neoplastic disease, the osteolytic involvement visualized is rather similar on both techniques. Additionally, in SBO, MRI allows for corroboration of the marrow involvement[1,17].

– Several authors have argued that ADC values in patients with bacterial SBO are usually higher than in those with a malignant neoplasm[1,4,18].
– Finally, if the imaging finding of a solid, contrast-absorbing mass at the base of the skull correlates with a clinically evident lesion, whether cutaneous or mucosal, the diagnosis of a neoplasm is greatly favored[4].

Below, we describe some examples of differential diagnoses:

– Nasopharyngeal carcinoma: this is the most common primary malignant neoplasm of the nasopharynx and is the main differential diagnosis for SBO. Some symptoms such as hearing loss, nasal obstruction, otalgia, headache, and cranial nerve involvement are often present in both conditions. Imaging findings may be indistinguishable when the changes are concentrated in the nasopharynx, making it difficult to discern whether the pathological process has spread downward toward the pharynx or upward toward the skull base. CT reveals a contrast-enhanced mass with aggressive behavior, with bone erosion and opacification of the mastoid air cells, while MRI also shows restricted diffusion with low ADC values, as previously mentioned[1,18]. Apart from the elements described, other elementary findings reported by Ozgen et al.[19] could support the diagnosis of a neoplasm when there are signs of lymph node dissemination, or of SBO when categorical abscesses are present (Fig. 9).
– Clival chordoma: this is an infiltrative tumor originating from extradural vestiges of the notochord. CT

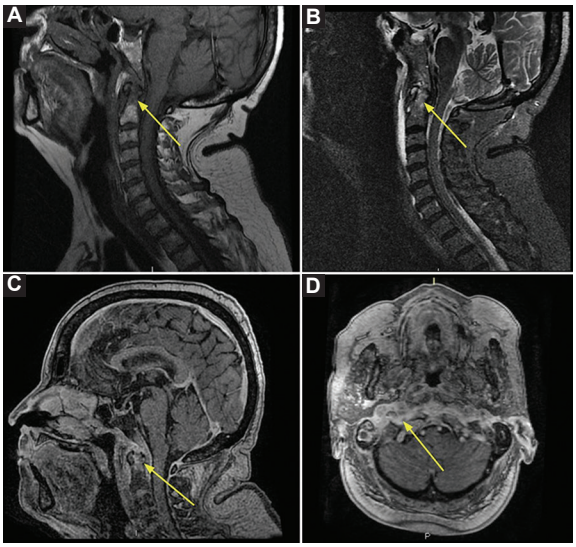

Figure 8. Bone marrow edema. A 71-year-old patient with a history of decompensated diabetes mellitus presented with symptoms of persistent subacute otic infection. MRI findings revealed T1 hyposignal of the bone marrow at the level of the odontoid process and the inferior part of the clivus (arrow in **A**), these same areas showed hypersignal on STIR sequences (arrow in **B**) and hyperenhancement on post-gadolinium T1-weighted images (arrow in **C**), indicating bone marrow edema. These alterations occurred in the context of a right otomastoid infection that spread to the prevertebral soft tissues and the craniocervical junction, with heterogeneous hyperenhancement of these anatomical regions on post-gadolinium sequences, consistent with phlegmonous changes (arrow in **D**).

shows a mass located in the midline at the level of the clivus, with osteolysis and bone remnants within its thickness. MRI typically shows high T2 signal with possible hypointense septa and low signal on the T1 sequence after contrast.

– Chondrosarcoma: it usually originates in the petroclival synchondrosis and is therefore located more laterally at the base of the skull. CT reveals a chondroid matrix (a "rings and arches" pattern of calcifications) mass with aggressive characteristics, mainly due to bone destruction. Non-mineralized areas usually show a dense or fluid signal, with facilitated diffusion on MRI. Contrast-enhanced images show heterogeneous enhancement, ranging from mild to intense, with a possible peripheral and septal pattern.
– Immunoglobulin G4 (IgG4)-related disease: this is a multisystem disease characterized by fibroinflammatory infiltration of various organs. It has a predilection for head and neck structures, including conditions such as idiopathic orbital inflammatory disease, orbital myositis, hypophysitis, hypertrophic pachymeningitis, dacryoadenitis, and vasculitis. However, it can also present as an isolated mass at the base of the skull. On CT, it appears as a soft tissue mass with bone erosion, while on MRI, it presents iso- to hyposignal on both T1 and T2 sequences, with possible diffusion restriction due to dense lymphoplasmacytic infiltration[20,21]. The diagnosis is based on the involvement of typical anatomical sites, serum IgG4 concentrations, and primarily its specific histopathological and immunohistochemical characteristics[1].
– Granulomatosis with polyangiitis: corresponds to a small-vessel vasculitis associated with antineutrophil cytoplasmic antibodies. The sinonasal region is the most affected in the head and neck. Imaging reveals a destructive process that initially involves both the septum and nasal turbinates, that extends symmetrically toward the maxillary antrum and then to the rest of the paranasal sinuses. It is accompanied by nodular mucosal thickening with granuloma formation that characteristically presents with low signal intensity on T1 and T2 sequences, although they enhance after gadolinium administration[22]. Otic involvement is less frequent, and its most common clinical presentation is serous otitis media secondary to Eustachian tube obstruction. Imaging findings of the temporal bone include opacification of the middle ear and the mastoid air cells, as well as osteolytic involvement of the same. MRI reveals an effacement of the fat planes around the foramina of the skull base with possible cranial nerve involvement, the facial nerve being the most frequently affected in its mastoid and tympanic segments[19]. One of the main imaging elements of differentiation with SBO, ignoring the possible systemic involvement of vasculitis, is the absence of bone marrow edema.

Treatment

Given the potential severity of this condition, treatment is initiated early with broad-spectrum intravenous antibiotics, with beta-lactams, and particularly cephalosporins, being the most commonly used. Antifungals can also be used empirically when there are clinical and radiological elements that support the diagnostic hypothesis, the most commonly used being voriconazole for suspected aspergillosis and amphotericin B for mucormycosis. Intravenous treatment typically lasts 6 weeks and aims to control the acute phase of the infection and achieve a minimum concentration of antibiotic in the bone tissue. Subsequently antibiotic

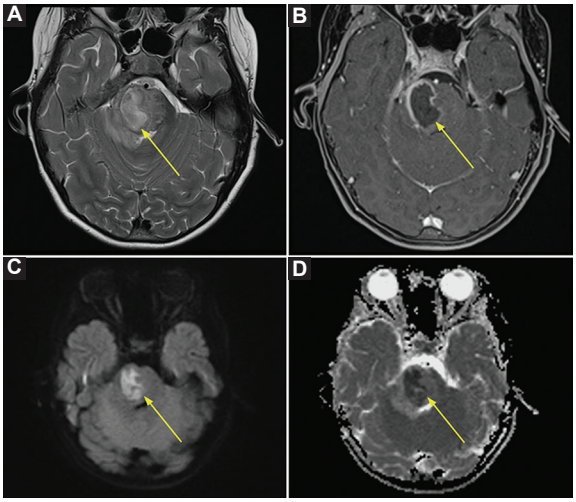

Figure 9. Brainstem abscess. Selected MRI sections of the clinical case in figure 6 show a right paramedian lesion at the level of the pons, with heterogeneous hypersignal on T2-weighted images (arrow in **A**), peripheral enhancement on post-gadolinium T1-weighted sequences (arrow in **B**), and restricted diffusion of its contents (arrows in **C** and **D**), consistent with an abscess. It is associated with phlegmonous tissue occupation of the cerebellopontine angle cistern and regional reactive pachymeningeal thickening.

treatment is continued orally, with a duration that varies depending on the patient's response.

Surgical debridement is often difficult and is reserved for specific cases, generally in extensive infections with abscess formation or involvement of vascular structures and cranial nerves. Other therapeutic aspects involve the control of diabetes and the use of anticoagulants in cases of associated venous sinus thrombosis[1,4,15].

In our series, the most commonly used antibiotics were cephalosporins, followed by ciprofloxacin, with treatments ranging from 4 to 14 weeks. In one particular case, a 6-year-old patient, required surgical drainage of a brainstem abscess that occurred as a complication of a typical SBO of otomastoid origin (Fig. 9). Patients with atypical SBO who presented with an invasive fungal infection due to Mucorales were treated with amphotericin B, combined with isavuconazole for coinfection with *A. niger*, in addition to surgical management with antrostomy and ethmoidectomy.

Conclusions and key points

SBO is a rare, potentially fatal, and difficult-to-diagnose condition. It should be considered in elderly diabetic or immunosuppressed patients who present a subacute condition with symptoms of a prolonged ear or rhinosinus infection. In the typical form, the infectious process has an otic origin and usually extends anteromedially through the extracranial soft tissues towards the petroclival region and the prevertebral musculature. In the atypical presentation, the initial focus is usually the rhinosinus, and the findings are primarily centered on the sphenoid bone, with spread of the infection to the middle and posterior cranial fossa, frequently affecting the clivus.

In SBO in general, and in cases caused by invasive fungal infection in particular, early clinical and radiological suspicion is crucial for the patient's survival. Correct interpretation of images requires an effective communication with the treating physician, allowing for consideration of clinical data and the physical examination in its evaluation.

Based on the analysis of the updated literature and our own case series, we can conclude that an adequate assessment of the extent of the disease requires complementary CT and MRI techniques, whose findings focus on four main elements: the primary infectious focus, phlegmonous changes in the extracranial soft tissues, bone marrow edema, and osteolysis.

The main differential diagnosis is neoplastic pathology, particularly nasopharyngeal carcinoma. On imaging, the presence of a dominant and reasonably measurable mass that alters the normal architecture of the tissue planes favors the diagnosis of a neoplasm. However, this differentiation is often not categorical based on clinical and radiological elements, and the histopathological study is mandatory.

Acknowledgments

The authors would like to thank their fellow imaging residents at the Universidad de Santiago de Chile, Dr. F. Venegas, and Dr. N. Aranda.

Funding

The authors declare that they have not received funding.

Conflicts of interest

The authors declare no conflicts of interest.

Ethical considerations

Protection of humans and animals. The authors declare that the procedures followed complied with the

ethical standards of the responsible human experimentation committee and adhered to the World Medical Association and the Declaration of Helsinki. The procedures were approved by the institutional Ethics Committee.

Confidentiality, informed consent, and ethical approval. The authors have obtained approval from the Ethics Committee for the analysis of routinely obtained and anonymized clinical data, so informed consent was not necessary. Relevant guidelines were followed.

Declaration on the use of artificial intelligence. The authors declare that no generative artificial intelligence was used in the writing of this manuscript.

References

1. Álvarez F, Barriga LQ, Iñigo TR, Roldán F. Diagnosis of skull base osteomyelitis. RadioGraphics. 2021;41:156-74.
2. Auinger AB, Dahm V, Stanisz I, Schwarz-Nemec U, Arnoldner C. The challenging diagnosis and follow-up of skull base osteomyelitis in clinical practice. Eur Arch Otorhinolaryngol. 2021;278:4681-88.
3. Vaidyanathan S, Kumar R. Imaging of acute and chronic skull base infection. Neuroimaging Clin N Am. 2021;31:571-98.
4. Chapman PR, Choudhary G, Singhal A. Skull base osteomyelitis: a comprehensive imaging review. AJNR Am J Neuroradiol. 2021;42:404-13.
5. Nguyen PT, Chang J, Shahlaie K, Raslan O, Ozturk A, Bobinski M, et al. Skull base infections, their complications, and management. Neuroradiol J. 2022;37:6-16.
6. Adams A, Offiah C. Central skull base osteomyelitis as a complication of necrotizing otitis externa: imaging findings, complications, and challenges of diagnosis. Clin Radiol. 2012;67:e7-e16.
7. Miranda-Merchak A, Kuschel C, Miranda M, Fuentes A. Anatomía radiológica de la base de cráneo y los nervios craneales parte 2: nervios craneales. Rev Chil Radiol. 2020;26:62-71.
8. Mazón M, Pont E, Montesinos P, Carreres-Polo J, Más-Estellés F. Radiología del oído externo: indicaciones, anatomía normal y procesos patológicos. Radiologia. 2016;58:189-98.
9. Mejzlík J, Černý M, Zeinerova L, Dědková J, Kopřiva J, Zadrobílek K, et al. The routes of infection spread in central skull-base osteomyelitis and the diagnostic role of CT and MRI scans. BMC Med Imaging. 2019;19:60.
10. Lanfermann H. Cranial neuroimaging and clinical neuroanatomy: atlas of MR imaging and computed tomography. 4th ed. New York: Thieme; 2019.
11. Bhalla D, Bhalla A, Manchanda S. Can imaging suggest the aetiology in skull base osteomyelitis? A systematic literature review. Pol J Radiol. 2021;86:309-21.
12. Djalilian HR, Shamloo B, Thakkar KH, Najme-Rahim M. Treatment of culture-negative skull base osteomyelitis. Otol Neurotol. 2006; 27:250-5.
13. Sokołowski J, Lachowska M, Karchier E, Bartoszewicz R, Niemczyk K. Skull base osteomyelitis: factors implicating clinical outcome. Acta Neurol Belg. 2019;119:431-7.
14. Johnson AK, Batra PS. Central skull base osteomyelitis. Laryngoscope. 2013;124:1083-7.
15. Khan MA, Quadri SAQ, Kazmi AS, Kwatra V, Ramachandran A, Gustin A, et al. A comprehensive review of skull base osteomyelitis: diagnostic and therapeutic challenges among various presentations. Asian J Neurosurg. 2018;13:959-70.
16. Aribandi M, McCoy VA, Bazan C. Imaging features of invasive and noninvasive fungal sinusitis: a review. Radiographics. 2007;27:1283-96.
17. Lesser FD, Derbyshire SG, Lewis-Jones H. Can computed tomography and magnetic resonance imaging differentiate between malignant pathology and osteomyelitis in the central skull base? J Laryngol Otol. 2015;129:852-9.
18. Ozgen B, Oguz KK, Cila A. Diffusion MR imaging features of skull base osteomyelitis compared with skull base malignancy. AJNR Am J Neuroradiol. 2010;32:179-84.
19. Park J, Karandikar A, Siu Cheng Loke T, Tan TY. Skull base osteomyelitis secondary to malignant otitis externa mimicking advanced nasopharyngeal cancer: MR imaging features at initial presentation. Am J Otolaryngol. 2017;38:466-71.
20. Huynh KN, Kong MJ, Nguyen BD. Anatomic and functional imaging of immunoglobulin G4–related disease and its mimics. RadioGraphics. 2023;43:e220097.
21. Sae C, Gye K, Young C, Kyung-Ja C, Chong S, Soo K, et al. Clinical and radiological features of diffuse lacrimal gland enlargement: comparisons among various etiologies in 91 biopsy-confirmed patients. Korean J Radiol. 2022;23:976-85.
22. Guzmán-Soto MI, Kimura Y, Romero-Sánchez G, Cienfuegos-Alvear JA, Candanedo-González F, Kimura-Sandoval Y, et al. From head to toe: granulomatosis with polyangiitis. RadioGraphics. 2021;41:1973-91.